NOVEL FOUR-DIMENSIONAL PRINTING OF 3D-PRINTED ABS VIA ELECTRON BEAM IRRADIATION

M.I. Shueb[1], M.E. Abd Manaf[2*], N. Mohamad[2], M. Mahmud[1] and A.M. Alkaseh[3]

[1]Radiation Processing Technology Division,
Malaysian Nuclear Agency,
Bangi, 43000 Kajang, Selangor, Malaysia.

[2]Fakulti Teknologi dan Kejuruteraan Industri dan Pembuatan,
Universiti Teknikal Malaysia Melaka,
Hang Tuah Jaya, 76100 Durian Tunggal, Melaka, Malaysia.

[3]Department of Training and Cooperation, Polymer Research Centre,
83152 Tripoli, Libya.

*Corresponding Author's Email: edee@utem.edu.my

Article History: Received 6 April 2024; Revised 14 November 2024; Accepted 16 November 2024

ABSTRACT: The proliferation of electronic devices has given rise to electromagnetic interference (EMI), which can cause malfunction in electronic devices and disrupt wireless communication systems. Polymers in their pure form exhibit limited EMI shielding properties due to their inherently low electrical conductivity. A promising approach to address this limitation is found in four-dimensional (4D) printing, which can manipulate the intrinsic characteristics of 3D-printed objects in response to external stimuli, such as electron beam (EB) irradiation. This paper investigated the effects of electron beam irradiation (0, 125, 250 kGy) on the thermal, electrical, and mechanical properties of 3D-printed ABS samples. In addition, it evaluates the influence of EB irradiation on the shielding effectiveness (SE). Both tensile strength and modulus showed a slight decrease with the increase of EB dosage. Contrarily, thermogravimetric analysis (TGA) results indicated an improvement in thermal stability with EB irradiation. EB irradiation causes polymer chains to undergo chain scission, where the polymer backbone is broken, leading to a decrease in the mechanical properties. While chain scission might reduce

tensile strength due to a weakened polymer structure, it may simultaneously increase thermal stability because shorter polymer chains are less susceptible to degradation at elevated temperatures. Moreover, a slight increase in SE value at a certain frequency is observed in the EB irradiated 3D-printed ABS. The increase in SE might be attributed to the decrease in porosity due to formation of crosslinked networks induced by EB radiation. The findings suggest that both crosslinking and chain scission take place upon EB irradiation of 3D printed ABS in this particular dosage range. Most significantly, this study demonstrates a promising method for improving the properties of 3D printed ABS intended for use in EMI shielding applications.

KEYWORDS: *4D Printing; ABS; Electron Beam Radiation; EMI Shielding*

1.0 INTRODUCTION

Electromagnetic interference, also known as EMI, is a phenomenon that can be defined as the transfer of disruptive electromagnetic radiation from one piece of electronic equipment to another through either the radiated, conducted, or both paths, resulting in difficulties with the operation of both pieces of equipment [1,2]. An undesirable EMI impact occurs when sensitive electronic equipment receives electromagnetic waves emitted by other electric or electronic devices. This impact can result in the system's failure and injury to the human body. Consequently, using EMI shielding materials is necessary to prevent EMI from causing functional disruption in electronic equipment. EMI shielding is the reflection and/or absorption of electromagnetic radiation by a substance, in which the material functioning as a shielding material prevents the penetration of high-frequency radiation.

Traditional EMI shielding products based on thermoplastic composites are generally manufactured using separate moulds at a specific temperature and pressure. The production process, therefore, is time-consuming and costly. In contrast, additive manufacturing (AM) technology enables the thin fabrication of intricate designs at a reduced cost and exceptional efficiency [3]. The AM process is a type of production that involves adding material in successive layers. This technology is ideal for producing products with intricate shapes that could not be manufactured using conventional machining processes. One of the currently available AM methods is fused deposition modelling (FDM). Nowadays, three-dimensional (3D) printing is one of the FDM processes widely known and utilized to manufacture 3D

components directly from the geometrical model generated in a CAD system. FDM-based 3D printing has become more cost-effective with the development of thermoplastic polymers such as acrylonitrile-butadiene-styrene (ABS) and polylactic acid (PLA) [4]. In a typical FDM process, thermoplastic polymer feedstock, often a filament, is heated to the glass transition temperature (T_g) and extruded through the 3D printer's nozzle, whose diameter determines the printing resolution. Computer-generated 3D models are constructed by successively adding layers of thermoplastic.

Acrylonitrile butadiene styrene (ABS) is a type of polymer variety widely used in 3D printing applications due to its unique structures and properties. Today, it has become an irreplaceable and universal substance with a critical impact on many industries. Nevertheless, the use of the 3D printed ABS does not completely satisfy the high-performance plastic class, hence significantly restricting its application. Novel investigations demonstrate that by adding electron-beam (EB) irradiation to the manufacturing process, the materials' properties may improve substantially. When irradiation is applied to a polymer matrix, active free radicals are produced due to the reaction. These radicals can enhance inter-chain interaction by creating C-C intermolecular bonds, allowing them to crosslink two long molecular chains. Up to a certain range of irradiation dose, the mechanical and thermal strength of the material improved [5].

EB irradiation could be a potent and straightforward technique for improving the mechanical properties of polymer composites through crosslinking [6]. It was found to be effective in improving interface compatibility, tensile strength, flexural strength, and thermal conductivity of ABS/Al_2O_3 composites [7]. However, it also decreases impact strength and thermal stability. The optimal radiation dose for improved overall performance is 30 kGy. They found that electron beam irradiation induces radiation-induced grafting and crosslinking reactions, forming stable crosslinked networks within the composites. It enhances the composites' interfacial adhesion and mechanical properties, increasing tensile and flexural strength.

Although limited research has explored the effects of EB irradiation on 3D-printed ABS, these studies have predominantly focused on specific dosage ranges, as highlighted in the works of Wady et al. [8] and Stuchebrov et al. [9]. A comprehensive understanding of how EB irradiation influences polymers across a spectrum of dosage levels is

vital for advancing the development of products and materials based on 3D-printed ABS. This study addresses this research gap by investigating the consequences of EB irradiation within the previously unexplored range of 125 – 250 kGy for 3D-printed ABS. This particular range has not been documented in prior research. In addition to comprehensive mechanical, physical, and thermal characterizations, the influence of EB irradiation on the material's shielding effectiveness is also evaluated. This study contributes valuable insights into the potential effects of EB dosage intensity on 3D-printed ABS, which can significantly inform the optimization of its properties for various applications.

2.0 METHODOLOGY

2.1 Materials

The 3D-printed ABS test pieces were made using a commercial 3D printing filament from Flash Forge, measuring 1.75 mm in diameter. The 3D-printed items were exposed to electron beam (EB) radiation at varying EB doses of 0, 125 and 250 kGy to generate 4D-printed objects by an external stimulus, as shown in Table 1.

Table 1: The EB irradiation doses applied for the 4D printing of the test pieces

Sample Name	EB Dose (kGy)
4DP-0	0
4DP-125	125
4DP-250	250

2.2 4D Printing of ABS via Electron Beam Irradiation

Firstly, the test piece drawings were created using AutoCAD. After the 3D models were drafted, the 3D files were exported into STL files before they were 3D printed. The samples were fabricated using a fused deposition modelling (FDM) 3D printing process using a 3D printer. The diameter of printer nozzle was set to 0.4 mm uniformly across the board to maintain consistency. The temperature of the printer nozzle was maintained at 215 °C during the whole operation, while the temperature of the printer build platform was maintained at 60 °C. The parameters for the printing were changed such that the printing speed was set at 50 mm/s, the layer thickness was set at 0.2 mm, and the line width was set at 0.2 mm.

As illustrated in Figure 1, 4D printing was performed by exposing the 3D printed samples to electron beam (EB) irradiation. The samples were

subjected to EB irradiation at an average dose rate of 15 kGy/s utilizing a 3 MeV electron beam. The dosages chosen were 125 and 250 kGy (Table 1). Following irradiation, the 4D-printed samples were immediately placed in hermetic plastic bags and stored at 2 °C before characterization.

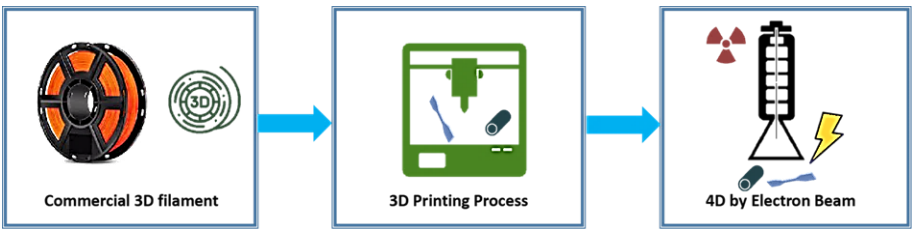

Figure 1: Conducting 4D printing via the exposure of a 3D printed sample to an electron beam

2.3 Testing and Characterization

2.3.1 Tensile Test

The tensile test of the 4D-printed samples was performed according to ASTM D638-Type 4 using the universal testing machine. The test sample was drawn at a 50 mm/min crosshead speed. Each composition underwent a total of five separate tensile tests to ensure reliability. Then, the resultant average values were calculated and documented.

2.3.2 FTIR

A Fourier transform infrared (FTIR) spectrophotometer was used to capture the FTIR spectra with a resolution of 4.0 cm^{-1} and in the wavenumber range of 4000 to 400 cm^{-1} to examine the change in the surface structure of 4D printing samples upon EB irradiation.

2.3.3 EMI Shielding Effectiveness

A vector network analyzer (VNA) was used to measure the EMI shielding effectiveness of the 4D-printed samples. Toroidal samples with an outer diameter of 6.95 mm and an inner diameter of 3.05 mm were employed for this purpose.

2.3.4 Thermal Analyses

Thermal characteristics of the 4D printed ABS samples were studied

using differential scanning calorimetry (DSC) and thermogravimetric analysis (TGA). For DSC measurement, nitrogen gas was used with a 50 mL/min flow rate to maintain an inert atmosphere. In order to remove thermal history, samples were first heated from −80 to 200 °C with a heating rate of 10 °C/min to, then cooled down to −80 °C at a cooling rate of 10 °C/min. Then, the samples were reheated to 200 °C at 10 °C/min. Meanwhile, TGA measurements were performed using a Pyrist 6 TGA analyzer by Perkin Elmer. The analysis enables us to investigate the effect of EB irradiation as an external stimulus on the thermal stability of 3D-printed ABS samples. The analysis was carried out at a heating rate of 10 °C/min from 30 to 600 °C. Nitrogen gas was utilized at a 20 mL/min flow rate to maintain an inert atmosphere.

2.3.5 Morphological analysis by FESEM

Field emission scanning electron microscopy (FESEM) was utilized for capturing the microstructure images of the samples. Before the morphological examination, the specimens were cut into smaller sizes of about 55 mm and coated with platinum using a Quarum Q150R S coater.

3.0 RESULTS AND DISCUSSION

3.1 Tensile Properties

Figure 2 demonstrates the ultimate tensile strength (UTS) of 3D printed ABS samples irradiated with different dosages of EB. UTS decreases almost monotonically with increasing irradiation dose.

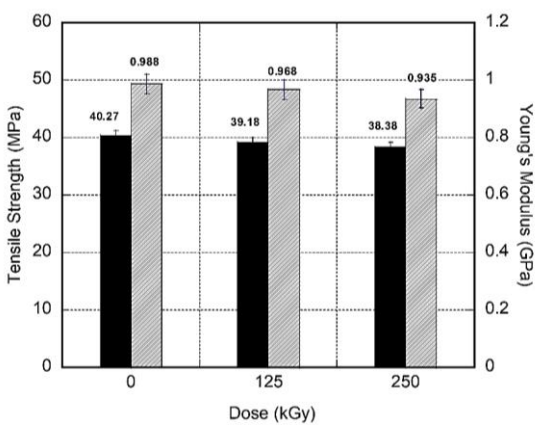

Figure 2: Impact of EB radiation dosage on tensile strength (left bar) and Young's modulus (right bar) of 3D printed ABS samples

The non-irradiated sample shows the highest tensile strength at 40.27 MPa. This result falls in the range of 3D-printed ABS reported elsewhere, around 30-45 MPa [10,11]. The tensile strength decreased by 2.71% to 39.18 MPa after the sample was irradiated at 125 kGy. When the irradiation dosage was increased to 250 kGy, the rupture stress was reduced by 4.69%, coming in at 38.38 MPa. High electron beam irradiation induces chain scissoring in the polymer matrix, considerably reducing tensile strength and elongation at break of the ABS samples [12]. Chain scissions and oxidative degradation were the primary processes that occurred during irradiation. Both of these processes decreased the material's molecular weight due to the generation of shorter chains and structures. It is well known that subjecting polymers to high-energy radiation will result in changes to the macromolecular structure of the polymer. These changes come about via the processes of competitive chain scission and crosslinking. According to the findings, irradiation influences the crystallinity and structure of polymers, which may change the performance of polymers.

3.2 FTIR

The examination of ABS transmittance using FTIR analysis reveals peaks between 2980 and 2800 cm^{-1}. These peaks are potentially caused by the stretching vibration of carbon-hydrogen (C-H) bonds. The evidence for this is the C-H bond deformation, as reported in some studies [13-15]. In addition, bending vibrations associated with the -CH_2 and CH_3 groups were detected at 1465 cm^{-1} and 1375 cm^{-1}, respectively. The energy at which the stretching vibration of the C=C peak can be observed is around 3010 cm^{-1} [7]. The peak observed at approximately 2250 cm^{-1} corresponds to the -C≡N functional group present in acrylonitrile within the ABS material [16]. By observing two distinct peaks at 750 cm^{-1} and 690 cm^{-1}, one can determine that the aromatic ring of styrene exhibits a mono-substitution pattern. High-energy electrons are projected into a gaseous medium, which frequently comprises water and oxygen molecules, in the process of electron beam radiation. The chemical effects induced by EB irradiation are responsible for these alterations. This procedure provides rise to reactive charged or ionized particles.

Based on the FTIR spectrum, it can be observed that as the electron beam dosage increased, the intensity of the -C-H stretching, CH_2-bending, and -CH_3 bending vibrations corresponding to wavenumbers

2940 cm^{-1}, 1450 cm^{-1}, and 1375 cm^{-1}, respectively, jumped. The observed phenomenon can be ascribed to the chain scission of ABS polymer. Crosslinking butadiene chains may have produced -C-C-bonds, as indicated by the increase in the stretching vibration of the -CH- group. Moreover, after subjecting ABS to electron beam with dosages of 125 kGy (4DP-125) and 250kGy (4DP-250), the intensity of the C=C peak remains unchanged. The prominent peak associated with the vibrational mode of -OH occurs between 3600 and 3100 cm^{-1}. The spectral range of 1690–1640 cm^{-1} exhibits the emergence of a novel broad peak attributed to the -C=N vibration subsequent to 125 kGy of irradiation. By increasing the dose to 250 kGy, the intensity of this apogee further escalates. It was observed that as the EB intensity increased during the experiment, the intensity of the peak corresponding to C≐N vibration at 2250 cm^{-1} decreased.

3.3 DSC

In FDM printing, printing materials must be heated above T_g and cooled to room temperature. Thus, T_g is the first and most essential parameter to be measured prior to any 3D modelling [17]. Table 2 shows the T_g value of commercially available unirradiated ABS filament (4DP-0), which is close to 106 °C. This figure went up to 107 °C for 4DP-125 after being exposed to 125 kGy of EB irradiation, and further increased to 109 °C after exposed to 250 kGy EB irradiation, in 4DP-250 sample. The melting temperature (T_m) and crystallization temperature (T_c) were not observed in the samples, indicating that they were fully amorphous. Radiation crosslinking is the probable cause for the increase in T_g. This result indicates that upon EB irradiation, the potential for molecular mobility decreases, and that greater energy is required to transition from the glass to the rubbery state. This decrease in molecular mobility may be associated to the decrease in free volume, due to the increased crosslinking in the system, which constrains the motion of the polymeric molecules. Because of the increased crosslinking, polymer chain mobility is decreased, leading to a lower free volume and, consequently, a greater T_g [18]. The increase in T_g value in the irradiated samples is consistent with the expected increase in crosslinking in the polymer's amorphous sections.

Table 2: Glass transition temperatures (T_g) of ABS sample under EB radiation during the second heating ramp

Sample	T_g (°C)
4DP-0	106.00
4DP-125	107.25
4DP-250	109.35

In the amorphous portion of the polymer, the crosslinking that occurred due to electron beam irradiation was responsible for the observed alteration in the properties [19,20]. The results of the DSC experiment provide more credence to the hypothesis that the crosslinking chain processes are the most important contributors to the radiation chemistry of ABS.

3.4 TGA

Thermal stability is mostly determined by bond energy. The polymer degrades as the temperature rises to the point where vibrational energy induces bond breaking. TGA analysis was thus performed to investigate the thermal stability characteristics of 4D printed materials. It is necessary for the heated constructed chamber, also known as an HBC, to reach a temperature high enough to liquefy the composites. On the other hand, if the temperature is raised too high, the components of the polymer may get damaged. TGA examined the thermal stability of the materials to ensure that the filaments would not disintegrate in the 3D printer's heated build chamber (HBC) and would remain stable rather than becoming brittle [17].

Under pyrolytic conditions in an N_2 atmosphere, the materials decomposed with a fast weight loss between 400 and 480 °C (Figure 3), followed by the formation of possible organic fragments (e.g. styrene, toluene, propenylbenzene, etc.). The onset temperature (T_{onset}) is defined as the temperature at which a testing sample loses 5% of its whole weight. From Figure 3, the T_{onset} of the samples is around 339.17 °C. As the HBC temperature was set to 230 °C, which is more than 100 °C below the T_{onset}, the polymer material turns into viscous and rubbery fluid instead of dissolving. The selected temperature was also sufficiently higher than the T_g of the ABS, allowing the filaments to pass through the 3D printer without issue. For T_g values between 104 and 110 °C, we can successfully avoid thermal deformation throughout the printing process by calibrating the heated build platform (HBP)

temperature 20 to 30 °C below T_g and maintaining the nozzle and HBC temperatures at 130 °C and 230 °C, respectively.

The thermograms and derivatograms (DTG) of 4DP-0, 4DP-125 and 4DP-250 are shown in Figures 6(a) and (b), respectively. The highest breakdown rate of 4DP-0 occurs at a temperature of 392 °C. In contrast, the maximum rate of decomposition of 4DP-125 and 4DP-250 takes place at 399 °C and 413 °C, respectively. Hence, it is possible to conclude that the initial and maximum rate of thermal degradation of the irradiated 3D-printed ABS takes place at a greater temperature than the unirradiated material. In other words, the thermal stability of the 4DP-125 and 4DP-250 is improved compared to their unirradiated counterparts, which is consistent with findings documented by Barkoula et al. [21]. The improved thermal stability of 4D-printed ABS might be related to the development of three-dimensional network upon irradiation by EB, which is caused by the crosslinking of the ABS chains. Improvement of thermal stability owing to crosslinking is further supported by higher values of maximum degradation temperature and lower rates of deterioration of 4D-printed samples, as evident in Figure 3.

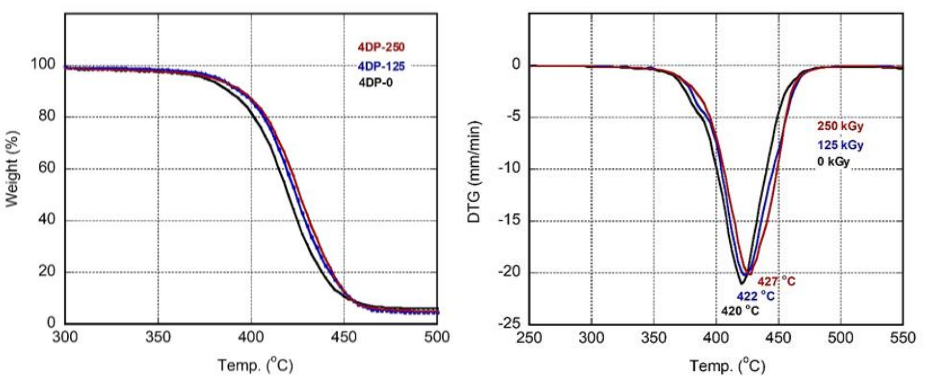

Figure 3: TG curves (a) and DTG (b) of unirradiated and irradiated 4D-printed ABS as a function of temperature

3.5 EMI Shielding Effectiveness

The electromagnetic interference (EMI) shielding performance of 4D printed ABS with 125 kGy (4DP-125) and 250 kGy (4DP-250) EB irradiation is depicted in Figure 4. The EMI shielding of the 4D printing samples was improved by 125 kGy and 250 kGy EB irradiation of the 3D-printed ABS polymer. It has been reported that the porosity of a

polymer created by applying 3D printing technology can affect the material's EMI shielding effectiveness [22]. The formation of strong crosslinks makes the polymer less porous. This observation agrees with the morphological analysis using FESEM. The irradiated samples possess a lower porosity than the control samples. This is due to the fact that high crosslinks tend to reduce the size of pores that connect them and the capillary structure [23]. At 8 GHz and 9 GHz, the 4D printed ABS demonstrated an increase in EMI shielding effectiveness from 2.8 and 1.87 dB to 3.45 and 4.10 dB, respectively.

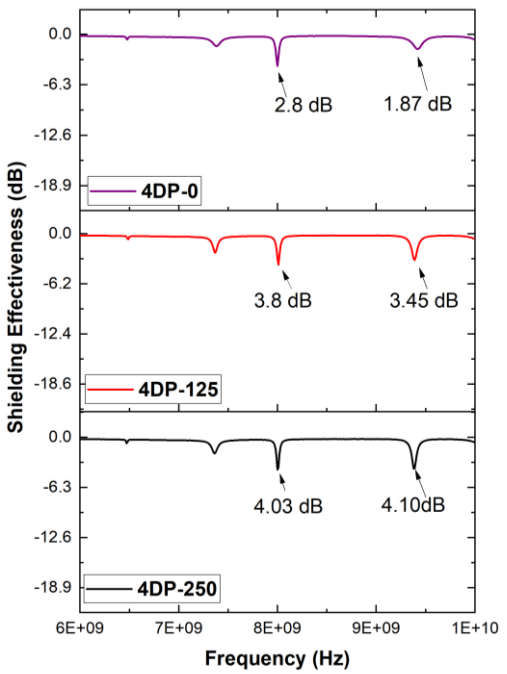

Figure 4: EMI shielding effectiveness of 4D-printed ABS at different EB dosages

3.6 Morphological Analysis

Figure 5 illustrates the FESEM images of the top surface of 4D-printed ABS layers. It is evident that the top surface of the membrane exhibited porous structures prior to irradiation as shown in Figure 5(a). However, upon EB irradiation, the introduction of robust crosslinks in 4DP-125 and 4DP-250 resulted in a notable reduction in the polymer's porosity. Over-crosslinking tends to reduce the size of the apertures that connect them to the capillary network [23].

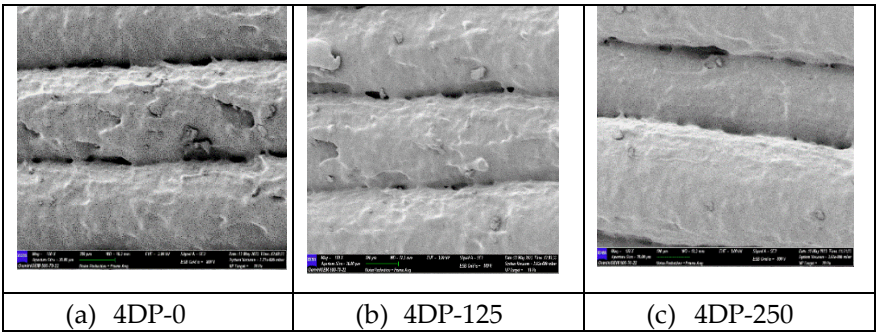

(a) 4DP-0 (b) 4DP-125 (c) 4DP-250

Figure 5: FESEM images of 4D-printed ABS samples at different EB dosages: (a) 0 kGy, (b) 125 kGy and (c) 250 kGy

3.7 Color Changes

Figure 6 displays photographic examples of discolored plastics due to the irradiation levels. The 4DP-250 sample appears slightly yellowish compared to the other samples. The discoloration or yellowish indicates the degradation level or radiation damage experienced by the samples. Radiation damage can lead to discoloration in specific polymer systems. This knowledge can be harnessed for opportunistic dosimetry, helping to determine the optimal timing for replacing printed materials. The alteration in hue may be influenced by either chemical activity or exposure to electron beams. The material's deposition density is subject to multiple factors associated with the printing process. It is evident that radiation-induced discoloration is linked to areas of increased porosity, while regions with higher density exhibit reduced color changes. This observation supports the hypothesis that radiation-induced chemical alterations are significantly influenced by the transportation of oxygen, hence the formation of pores, and the printing pattern [20].

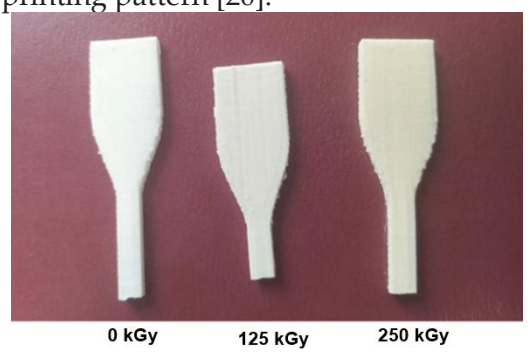

Figure 6: Color changes of the EB irradiated 3D-printed ABS at different EB dosages: (a) 0 kGy, (b) 125 kGy and (c) 250 kGy

4.0 CONCLUSION

In this work, EB irradiation in the range of 125–250 kGy was performed on 3D-printed ABS to obtain 4D-printed ABS. The structural properties, thermal stability, and EMI shielding of the 4D-printed ABS were discussed comprehensively. It was discovered that 4D printing with EB irradiation produced materials with improved thermal stability, structural properties, and EMI shielding effectiveness. The EB irradiation causes chain scission and crosslinking in the polymer, leading to a decrease in tensile strength but an increase in thermal stability. The EMI shielding effectiveness of the 4D-printed ABS is also enhanced due to the reduction in porosity caused by the formation of crosslinked networks. This research demonstrates the potential of EB irradiation for enhancing the properties of 3D-printed ABS for various applications.

ACKNOWLEDGEMENTS

The authors would like to thank the Malaysian Nuclear Agency and the Fakulti Teknologi dan Kejuruteraan Industri dan Pembuatan of UTeM for providing the equipment and technical support which made this work possible.

AUTHOR CONTRIBUTIONS

M.I. Shueb: Conceptualization, Methodology, Original Draft Preparation; M.E. Abd Manaf: Validation, Final Editing; N. Mohamad: Methodology; M. Mahmud: Methodology; A.M. Alkaseh: Validation.

CONFLICTS OF INTEREST

The article has not been published elsewhere and is not under consideration by other journals. All authors have approved the review, agreed with its submission, and declared no conflict of interest on the article.

REFERENCES

[1] L. Omana, A. Chandran, R.E. John, R. Wilson, K.C. George, N.V. Unnikrishnan, S.S Varghese, G. George, S.M. Simon and I. Paul, "Recent

advances in polymer nanocomposites for electromagnetic interference shielding: a review", *ACS Omega*, vol. 7, no. 30, pp. 25921-25947, 2022.

[2] M.I Shueb, M.E.A. Manaf, J.A Razak, N. Mohamad, K.N.K. Umar and V.A. Doan, "Enhancing the electrical conductivity of nylon 66 via the incorporation of silane-functionalized graphene nanoplatelets", *Journal of Advanced Manufacturing Technology*, vol. 17, no. 2, pp. 17-29, 2023.

[3] H. Luo, Y. Tan, F. Zhang, J. Zhang, Y. Tu and K. Cui, "Selectively enhanced 3D printing process and performance analysis of continuous carbon fiber composite material", *Materials*, vol. 12, no. 21, pp. 1-14, 2019.

[4] M.R. Skorski, J.M. Esenther, Z. Ahmed, A.E. Miller and M.R. Hartings, "The chemical, mechanical, and physical properties of 3D printed materials composed of TiO2-ABS nanocomposites", *Science and Technology of Advanced Materials*, vol. 17, no. 1, pp. 89-97, 2016.

[5] N. Talip, A.M. Afifi, M.Y. Hamzah, M. Mahmud and S. Idris, "Radiation modified CS/PVA film with PVP coating as Cu adsorbent material", *Pertanika Journal of Science & Technology*, vol. 29, no. 2. pp. 1119-1134, 2021.

[6] V. Phetarporn, S. Loykulnant, C. Kongkaew, A. Seubsai and P. Prapainainar, "Composite properties of graphene-based materials/natural rubber vulcanized using electron beam irradiation", *Materials Today Communications*, vol. 19, pp. 413-424, 2019.

[7] D. Guo, L. Li, Q. Chen, L. Tu, B. Wu, C. Luo, W. Lv, Z. Xu, H. Yang, Z. Liao and Y. Chen, "Simultaneous improvement of interface compatibility and thermal conductivity for thermally conductive ABS/Al2O3 composites by using electron beam radiation processing", *Journal of Polymer Research*, vol. 28, no. 7, pp. 1-8, 2021.

[8] P. Wady, A. Wasilewski, L. Brock, R. Edge, A. Baidak, C. McBride, L. Leay, A. Griffiths and C. Valles, C., "Effect of ionising radiation on the mechanical and structural properties of 3D printed plastics", *Additive Manufacturing*, vol. 31, pp. 1-29, 2020.

[9] S.G. Stuchebrov, A.A. Bulavskaya, Y.M. Cherepennikov, A.A. Grigorieva, I.A. Miloichikova, N.E. Toropkov and M.V. Shevelev, "Changes in the physical and structural properties of 3D-printed plastic samples under radiation exposure by nearly therapeutic dose", *Journal of Instrumentation*, vol. 15, no. 04, pp. 1-11, 2020.

[10] T. Vukasovic, J.F. Vivanco, D. Celentano and C. García-Herrera, "Characterization of the mechanical response of thermoplastic parts fabricated with 3D printing", *The International Journal of Advanced Manufacturing Technology*, vol. 104, pp. 4207-4218, 2019.

[11] J.T. Cantrell, S. Rohde, D. Damiani, R. Gurnani, L. DiSandro, J. Anton, A. Young, A. Jerez, D. Steinbach, C. Kroese and P.G. Ifju, "Experimental characterization of the mechanical properties of 3D-printed ABS and polycarbonate parts", *Rapid Prototyping Journal*, vol. 23, no. 4, pp. 811-824, 2017.

[12] S.T. Bee, L.T. Sin, C.T. Ratnam, W.S. Chew and A.R. Rahmat,

"Enhancement effect of trimethylopropane trimethacrylate on electron beam irradiated acrylonitrile butadiene styrene (ABS)", *Polymer Bulletin*, vol. 75, pp. 5015-5037, 2018.

[13] J. Li, F. Chen, L. Yang, L. Jiang and Y. Dan, "FTIR analysis on aging characteristics of ABS/PC blend under UV-irradiation in air", *Spectrochimica Acta Part A: Molecular and Biomolecular Spectroscopy*, vol. 184, pp. 361-367, 2017.

[14] M.R. Jung, F.D. Horgen, S.V. Orski, V. Rodriguez, K.L. Beers, G.H. Balazs, T. Jones, T.M. Work, K.C. Brignac, S.J. Royer and K.D. Hyrenbach, "Validation of ATR FT-IR to identify polymers of plastic marine debris, including those ingested by marine organisms", *Marine Pollution Bulletin*, vol. 127, pp. 704-716, 2018.

[15] A.J. Miller, G.M. Warner and D. Raghavan, "Proton radiation effects on the mechanical and chemical characteristics of 3D printed ABS: Preliminary results", *Transactions of the American Nuclear Society*, vol. 122, pp. 253-256, 2021.

[16] J.V.B. Silveira, M.F.D. Aguiar, J.J. Silva, C.P.D. Melo, C.A. Andrade, A.G. Silva-Junior, H.P.D. Oliveira and K.G. Alves, "Substrate coating produced via additive manufacturing with conducting polymers: Assessment in the development of electrodes", *Materials Research*, vol. 26, pp. 20220524, 2023.

[17] X. Wei, D. Li, W. Jiang, Z. Gu, X. Wang, Z. Zhang and Z. Sun, "3D printable graphene composite", *Scientific Reports*, vol. 5, no. 1, pp. 1-7, 2015.

[18] F. Dong, S. Maganty, S.J. Meschter, S. Nozaki, T. Ohshima, T. Makino and J. Cho, "Electron beam irradiation effect on the mechanical properties of nanosilica-filled polyurethane films", *Polymer Degradation and Stability*, vol. 141, pp. 45-53, 2017.

[19] E. Adem, G. Burillo, L.F. Del Castillo, M. Vásquez, M. Avalos-Borja and A. Marcos-Fernández, "Polyamide-6: The effects on mechanical and physicochemical properties by electron beam irradiation at different temperatures", *Radiation Physics and Chemistry*, vol. 97, pp. 165-171, 2014.

[20] C. Mastalerz, I. Vroman, X. Coqueret and S. Alix, "Effects of electron beam irradiation on 3D-printed biopolymers for bone tissue engineering", *Journal of Composites Science*, vol. 5, no. 7, pp. 182, 2021.

[21] N.M. Barkoula, B. Alcock, N.O. Cabrera and T. Peijs, "Flame-retardancy properties of intumescent ammonium poly (phosphate) and mineral filler magnesium hydroxide in combination with graphene", *Polymers and Polymer Composites*, vol. 16, no. 2, pp. 101-113, 2008.

[22] A.K. Singh, A. Shishkin, T. Koppel and N. Gupta, "A review of porous lightweight composite materials for electromagnetic interference shielding", *Composites Part B: Engineering*, vol. 149, pp.188-197, 2018

[23] R.H. Moghaddam, S. Dadfarnia, A.M.H. Shabani, Z.H. Moghaddam and M. Tavakol, "Electron beam irradiation synthesis of porous and

non-porous pectin based hydrogels for a tetracycline drug delivery system", *Materials Science and Engineering: C*, vol. 102, pp. 391-404, 2019.